INTERNATIONAL JOURNAL OF INNOVATIVE RESEARCH & DEVELOPMENT

ISSN 2278 – 0211 (Online)

In-vitro Interaction of αB-Crystallin on Serum Amyloid a and Serum Amyloid a Fibrils with Neuro 2a Cells

Asokan C.
Professor, Department of Biochemistry,Sokoto State University, Sokoto, Sokoto State, Nigeria
Musthapha I.
Assistant Lecturer, Department of Biochemistry, Sokoto State University, Sokoto, Sokoto State, Nigeria

Abstract:
The interactions of SAA and SAA protofibrils with protecting role of alphaB-Crystallin with neuro 2a cells of the mouse are dealt with in detail to study the binding of SAA protofibrils in various conditions. Specifically, interaction of serum amyloid A fibrils with a cell surface binding site/receptor might alter the local environment to cause cellular dysfunction and to be more favorable for amyloid formation and prevention. This is important in relation to the activity of membrane proteins, because losing the activity of such systems will ultimately lead to malfunction or death of the cell. The interactions of Serum Amyloid A (SAA) and Serum Amyloid A protofibrils with neuro 2a cells of the mouse are dealt with in detail to study the binding of SAA protofibrils in various conditions. The induced fluorescence, induced circular dichroism, FACScan and MTT assay results have shown the SAA and SAA prototfibrils binding and cell toxicity with the neuro 2a cells with different concentrations of alphaB-Crystallin 0.15-15 nM. Specifically, cells were incubated with 1.25-6.25 μM SAA-FITC and SAA protofibrils-FITC assayed. The 50% viable neuro 2a cells at 4–6 μM with an LD_{50} of 3.5 μM. The interaction of serum amyloid A fibrils with a cell surface binding site/receptor might alter the local environment to cause cellular dysfunction and to be more favorable for amyloid formation. In the present study, concluding that the SAA fibrils and SAA protein binding and neuro 2a cell cytotoxicity was reduced in the presence of alphaB-Crystallin.

Keywords: *Serum Amyloid A, Crystallin, Neuro 2a Cells, FITC, Fibril, Protofibril.*

1. Introduction

Small heat-shock proteins (sHSPs) are one of four families of heat-shock proteins (HSPs) expressed in response to heat shock and other forms of stress (Parsell and Lindquist 1993). They are a diverse family of proteins that appear to be ubiquitous in nature, being found as surface antigens in eukaryotic parasites, as inclusion body-binding protein in E. Coli, and as structural proteins in the vertebrate lens (Caspers et al 1995). Despite their low molecular mass (12-40 kDa), sHSPs are isolated as large oligomeric complexes of 2-40 subunits depending on the physiological state of the cell. Distant members of the family have relatively low sequence similarity except for a highly conserved stretch of 100 amino acids, often called the α-Cyrstallin domain (Caspers et al 1995). Although their cellular function under physiological conditions is still largely unknown, the increased expression of sHSP is associated with cell survival under heat stress (Arrigo and Landry 1994). The role of these proteins in thermotolerance appears to be a consequence of their ability to function as molecular chaperones and to modulate actin filament dynamics (Lee et al 1995). sHSPs from many species inhibit the unfolding-induced aggregation of proteins in an ATP-independent manner and form a stable complex with their protein substrate. Thus, during periods of stress, sHSPs act as energy-independent traps preventing the irreversible aggregation of proteins. Recently, it has been shown that upon establishment of refolding conditions, proteins bound to sHSPs are efficiently refolded in cooperation with other chaperones (Lee et al 1997)

α-Crystallin is one of the heat shock proteins and its chaperonic activity is well established. α-Crystallin forms complexes with denaturing proteins, thereby preventing their uncontrolled aggregation. Chaperonine process has been shown to follow a saturation type of complexing, i.e., when the ability of the available α-Crystallin to bind the target protein is exceeded, the excess target protein aggregates and eventually precipitates out of solution (Bettelheim et al 1999). In other chaperone forms the existence of such equilibrium has been demonstrated (Walter et al 1996). In the small heat shock chaperones (e.g., Hsp 25), to which α-Crystallin belongs, the assumption is that they do not release proteins once complexed (Creighton and Jaenicke 1993). However recent results suggest that they do shift the equlibrium *in-vitro* via secondary interaction of the high molecular weight complex with Hsp 70

(Ehrnsperger et al 1999). With α-Crystallin there is a lack of experimental evidence to indicate whether the association of partially denatured α-lactalbumin with α-Crystallin is a reversible or irreversible process. Lindner et al. (1997) studied the interaction of α-Crystallin with α-lactalbumin by proton NMR spectroscopy. They have shown that α-Crystallin interacts only with the molten globule state of α-lactalbumin along the denaturation pathway. Such molten globule states are in equilibrium with the folded protein. According to them, α-Crystallin interacts with the large hydrophobic surface of the molten globule form of α-lactalbumin and stabilizes them that shift the equilibrium away from aggregation. It is not known whether such a complex can release the unfolded α-lactalbumin. Recently, in a similar system, DTT denatured lysozyme, chaperoned by α-Crystallin, interacted only with the irreversibly destabilized form of lysozyme.

Mitochondrial fusion and fission proteins were notably dysregulated by Aβ42 (Mfn1) or Aβ42 plus ceramide (OPA1, Drp1). Antioxidant vitamins blocked the Aβ42 alone-induced ROS production, but did not reverse Aβ42-induced ATP reduction or complex IV inhibition. Aβ expression combined with ceramide exposure had additive effects to decrease cell viability (Gamache et al 2015). Endogenous Grb2 partially co-localizes to late endosomal compartments along with AbetaPP and AbetaPP intracellular domain (AICD) "adaptor" protein, growth factor receptor protein binding protein 2 (Grb2). Increase in the concentration of Grb2 confines it in enlarged late endosomes leading to more sequestration of AbetaPP and AICD within these compartments. This confinement of AbetaPP due to Grb2 overexpression affects its turnover by inhibiting its release via exosomal vesicles. As a consequence, the level of intracellular AbetaPP and AICD increases (Raychaudhuri and Mukhopadhyay 2010). Earlier studies reveal the significance of a specific interaction of the two molecules to optimize the rapid transport of AICD inside endosomal vesicles presumably to reduce the cytotoxic load (Das et al 2011). Prolyl oligopeptidase (PREP) inhibitors may reduce accumulation of alphaSyn inclusions via a dual mechanism and are thus a novel therapeutic candidate for synucleinopathies (Savolainen et al 2015).

The role of αB-Crystallin in the development of these diseases is largely unknown but may be related to its functional role as a small heat shock protein (Caspers et al 1995). Recently, α-Crystallin was reported to act as a chaperone molecule capable of protecting other proteins from denaturation (Horwitz 1993). Whether this chaperone function is active in-vivo either in the lens, or, in other tissues, is unknown. To understand the effect of αB-Crystallin on Aβ fibril formation, we need to determine whether they interact with each other. In the present study, in-vitro studies on the role of the interaction of SAA/SAA fibrils with chaperones were investigated. The results indicated that there was interaction between SAA and αB-Crystallin when they were incubated together with neuro 2a Cells. A possible mechanism for this interaction and its implicated significance in-vitro are discussed.

2. Materials and Methods

2.1. Isolation of αB-Crystallin

Bovine lenses (8-10 lenses) were decapsulated and homogenized (Luthra and Balasubramanian 1993) in 0.1 M Tris buffer, pH 7.4 containing 0.5 M NaCl, 1 mM EDTA, and 0.1% NaN_3. The insoluble protein fraction and membrane debris was removed by centrifugation at 30,000g for 30 min. The supernatant was chromatographed on a Sephacryl-S200 (Pharmacia Biotech, Uppsala, Sweden) gel filtration column (0.8 × 90 cm) to separate the alphaB-Crystallin using Gradifrac™ FPLC system (Pharmacia Biotech, Uppsala, Sweden). Each of the alphaB-Crystallin fractions was dialyzed repeatedly against water using FILTRON concentrating 10000 D. Molecular weight cut off membrane (Gelman Sciences, India) and lyophilized and stored at -20°C. Protein was determined by Lowry et al (Lowry et al 1951). Homogeneous 12% SDS-polyacrylamide gels were run on the mini gel electrophoresis system (Laemmli, 1970).

2.2. Isolation of SAA

SAA was isolated from the plasma of casein injected (Botto et al 1997) mice as reported previously by Lindhorst et al (Lindhorst et al 1997). It was then characterized using 17% SDS-polyacrylamide gels. Isolated SAA was purified by Waters reverse phase-high performance liquid chromatography (Kaplan et al 1999) (RP-HPLC) analytical column 4.6 × 250 mm Spherisorb ODS2 LC_{18} (Waters, Milford, Massachusetts, USA) and size exclusion chromatography (SEC) columns using a series of 7.8 × 300 mm Ultrahydrogel 250™ and Ultrahydrogel 500™ the molecular weight was determined (Waters, Milford, Massachusetts, USA).

2.3. Fluorolabelling of SAA and SAA fibrils

Purified SAA and SAA proptofibrils (400 µg/400 µl 0.001% NH_4OH, pH 9.0) were labeled with fluorecein isothiocyanate (FITC) (Fluka, USA) by dialysis through a 1000 D cutoff membrane. FITC (0.4 mg) was dissolved in 40 µl DMSO and added to 40 ml of PBS adjusted to pH 9.0 with NH_4OH. After 12 hrs at 4°C the SAA-FITC and SAA protofibrils-FITC were dialyzed against milli-Q water, sterile filtered (0.45 µm) and held at 4°C (Linke et al 1991). 1.25-6.25 µM of SAA-FITC and SAA protofibrils-FITC were assayed with 0.15-15 nM of αB-Crystallin.

2.4. Single Photon Counting Life-time Measurements

1.25-6.25 µM of SAA-FITC and SAA protofibrils-FITC was assayed with 0.15-15 nM of αB-Crystallin for lifetime measurements (FL, at λ_{max} 530±15 nm) (Spectra physics, IBH Consultants, Scotland, UK).

2.5. Induced Circular Dichroic Spectroscopic Studies

1.25-6.25 μM of SAA-FITC and SAA protofibrils-FITC were assayed with 0.15-15 nM of αB-Crystallin for induced CD measurements (Jasco J-715 Spectropolarimeter, Tokyo, Japan).

2.6. FACScan Analysis: Neuro 2a Cells

Mice neuro 2a cells were incubated with 1.25-6.25 μM of SAA-FITC and SAA protofibrils-FITC assayed with 0.15-15 nM of αB-Crystallin for 24 hrs at 4°C, washed in PBS, fixed immediately in 1% paraformaldehyde in PBS, and assayed for cellular fluorescence (FL, at λ_{max} 530±15 nm), forward scatter (FSC), and side scatter (SSC). Binding was analyzed on a FACScan flow cytometer using FACScan analysis software WINMDI (Becton Dickinson, San Jose, CA, USA).

2.7. MTT Assay

1.25-6.25 μM of SAA-FITC and SAA protofibrils-FITC were assayed with 0.15-15 nM of αB-Crystallin (Rousset 2001) for incubation with neuro 2a cells for 24 hrs. neuro 2a cells were fed with 200 μL fresh medium at the ends of the growth period and added 50 μl of MTT to all wells in columns 1 to 6. Wrapped plates in aluminum foil and incubated for 4 hrs in a humidified atmosphere at 37°C. This is a minimum incubation time and plates can be left for up to 8 hrs. Removed the medium and MTT from the wells and dissolved the remaining MTT-formazan crystals, adding 200 μl of DMSO to all wells in columns 1 to 6. Added glycine buffer (25 μl per well) to all wells containing the DMSO. Recorded absorbance at 570 nm immediately, since the product was unstable. The wells in column 1, which contained medium, MTT, but no cells, were used to blank the plate reader.

3. Results

The fluorescence spectral changes observed on αB-Crystallin binding to FITC-SAA was shown in spectrum Fig. 1a. During addition of αB-Crystallin, the fluorescence at 516 nm decreased gradually indicating that FITC-fluorescence was quenched by the disulfide bonds in αB-Crystallin. The fluorescence intensity was increased during addition of αB-Crystallin to SAA protofibril-FITC. This increase in FITC intensity may be associated with the conversion of protofibrils by αB-Crystallin in lower concentration (at 5 nM). However, further addition of αB-Crystallin does not change the fluorescence intensity. The effect of αB-Crystallin concentration on lifetime of FITC-SAA protofibril is indicated in Fig. 1b.

The average fluorescence lifetime decreased from 3.0 to 1.2 ns indicating that the flourophore is in highly polar environment than the previous state. In high αB-Crystallin concentration (30 nM), there was quenching of FITC in SAA by disulfide groups around the environment. The amplitude for long lifetime (τ_1) was decreased significantly from 50% to 40% during addition of αB-Crystallin. However, short-lived species was constant during further αB-Crystallin incubation (Fig. 2a and b).

From the induced CD studied, changes in FITC environment of SAA were measured at different concentrations of αB-Crystallin. The CD band at 450 and 505 nm were changed during addition of αB-Crystallin. The measured ellipticity values were plotted against various concentrations of αB-Crystallin which, is given in Fig. 3a. The ellipticity attained saturation at 2 nM αB-Crystallin. Further addition of αB-Crystallin did not change the ellipticity at 505 nm. FITC labeled SAA protofibril also showed similar effect on addition of αB-Crystallin. The CD band at 450nm gradually decreased as a function of αB-Crystallin (Fig. 3b). The negative band at 505 nm increased even at very low concentration of αB-Crystallin. Further addition (7.5 nM) did not change the ellipticity significantly.

Flow cytometry revealed that the SAA-FITC positive binding readily occurred in the presence of αB-Crystallin in neuro 2a brain cells and is shown in histograms. Both mean fluorescence intensity, as well as percentage of positive cell increased as a function of αB-Crystallin. However, the binding of SAA-FITC was almost completely prevented by simultaneous addition of αB-Crystallin. The histogram (Fig. 4a) showed the decrease in the percentage of positive binding than in the FITC-SAA control experiment during addition of αB-Crystallin. The mean fluorescence intensity was decreased to 45% of control values 55% in neuro 2a cells, respectively (Fig. 4a). The cell volume and granulating changes were also studied by using forward and side scatter plot. In neuro 2a cells studied the forward scatter values were not varied significantly indicating that the volume of cells remain constant during αB-Crystallin addition. However, Side scatter values were increased significantly indicating that the αB-Crystallin treated cells were highly granular (Fig. 4b, c and d).

We next studied the cellular binding of SAA protofibril-FITC in the presence of various concentration of αB-Crystallin. The SAA protofibril-FITC binding to neuro 2a cells decreased markedly during the addition of αB-Crystallin. The mean fluorescence intensity decreased from 70% to 30% as shown in FL plot. From the histogram, the shifting of cell population from fluorescence positive region towards control cells (Fig. 5a) is seen. Further the cell cytotoxicity studies were carried out by MTT assay.

4. Discussion

The principal role of SAA during the acute-phase reaction appears to be the association with HDL-particles and subsequent changes of apolipoprotein composition and metabolic properties of its physiological carrier. Because SAA may displace apolipoprotein A-I, the major apolipoprotein of HDL, it is hypothesized that SAA could alter the protective function of HDL during 'reverse cholesterol transport (Artl 2000). SAA binding acute phase reaction was studied with macrophages (representative peripheral cells) revealed that

the binding affinity for SAA is enhanced, earlier findings suggest that extracellular matrix proteins appear to serve as a temporary anchorage sites for SAA and amyloid A (Preciado-Patt et al 1996).

Earlier studies hypothesized that the biophysical characteristics of apoE4, notably domain interaction, affect its folding and, thus, its trafficking from the endoplasmic reticulum (ER) through the Golgi apparatus to the cell membrane. To test this hypothesis, we transfected Neuro-2a cells (Sato et al 2014) and mouse primary hippocampal neurons with cDNA constructs encoding enhanced green fluorescent protein (EGFP)-tagged apoE proteins (apoE3, apoE4, and apoE4-R61T) as a noninvasive probe to measure fluorescence recovery after photobleaching (FRAP), a powerful technology that can monitor intracellular trafficking of cargo proteins (Brodbeck et al 2011) .

The FITC fluorescence quenching ability of protein varies in proportion to disulfide groups. In monomeric SAA, addition of αB-Crystallin causes quenching of fluorescence. This clearly indicates that FITC environment in SAA is near to the disulfide groups of αB-Crystallin. However, the mechanism of binding of αB-Crystallin to SAA is still unknown. The SAA protofibril-FITC also interacts with αB-Crystallin resulting in enhanced fluorescence intensity. This is possibly due to exposure of FITC region of SAA to a more polar environment. In the case of the αB-Crystallin binding to protofibril, the FITC region is far away from the disulfide groups of αB-Crystallin. Decay of FITC labeled SAA showed multiple fluorescent lifetime species and addition of αB-Crystallin significantly decreased the average fluorescence lifetime of FITC. The decrease in lifetime of FITC is possibly due to the association of αB-Crystallin to the SAA. The interaction of disulfide groups in αB-Crystallin on FITC groups of SAA quenched the fluorescence of probe, which is accompanied by a decrease in fluorescence lifetime.

Primary neurons that were found with accumulated oligomeric Ab had lost branches and were degenerated, indicating that oligomeric Ab may cause neuronal degeneration. These findings suggest that in patients with AD, increased production of Ab and the interaction of Ab with Drp1 are crucial factors in mitochondrial fragmentation, abnormal mitochondrial dynamics and synaptic damage. Inhibiting, these abnormal interactions may be a therapeutic strategy to reduce mitochondrial fragmentation, neuronal and synaptic damage and cognitive decline in patients with AD (Manczak et al 2011).

From the induced CD studies, it is clear that the folding of SAA occurs up to 2 nM concentration of αB-Crystallin. Further addition of αB-Crystallin did not change the FITC region of SAA. However, in the protofibrils, FITC-environment changes were observed only upto 1 nM of αB-Crystallin. Futher addition of αB-Crystallin did not altered the conformation of FITC molecular environment indicating the completion of the folding process at low concentration of αB-Crystallin in protofibrillar than in native form of SAA. Studies explains that identification of BM88/Cend1 as a component of mature neurons several years ago, a clearer picture of its biology has emerged as a neuronal-specific regulator of cell cycle exit and differentiation of neuronal precursors in the developing nervous system. The study found that this molecule is expressed in CNS cells all along the neuronal lineage in a characteristic fashion: at low levels in neural stem/progenitor cells and at higher levels in post-mitotic differentiated neurons (Politis et al 2008).

Using flow cytometric studies, the competing nature of αB-Crystallin with monomeric and protofibrillar SAA binding was studied in neuro 2a cells. αB-Crystallin did not compete with monomeric SAA binding to neuro 2a cells. This is possibly due to the occurrence of a large number of high affinity SAA binding sites on neuro 2a cells. However, neuro 2a cells the SAA binding decreased in the presence of αB-Crystallin. This effect is either due to the presence of low affinity SAA binding site or competing effect of αB-Crystallin with SAA in the binding process. αB-Crystallin may prevent the SAA mediated toxic mechanism in neuro 2a cells.

Protofibril binding to neuro 2a cells significantly decreased in the presence of αB-Crystallin. This effect may be either due to αB-Crystallin complexation of SAA protofibrils. The αB-Crystallin incubation with SAA significantly increased the granularity in cell lines.

5. Conclusion

In conclusion, the interaction and binding of SAA protein and porotofibrils with neuro 2a cells decreases in the presence of αB-Crystallin and the cytotoxicity of the SAA and SAA protofibrils reduced.

6. Acknowledgements

We thank to Council of Scientific Industrial Research-Senior research fellowship, New Delhi. India. Dr. T. Ramasami,Director, Central Leather Research Institute, Chennai. India for his kind permission to publish this work. We are also thankful to Dr. A. Meenakshi, Cancer Institute, Chennai for her valuable help in fluorescence microscopy facility. We also thank Prof. Ramurthy, University of Madras, and Chennai for his kind permission to use fluorescence spectroscopy and single photon counting facility.

7. References

i. Arrigo, A. P. and Landry, J. The biology of heat-shock proteins and molecular chaperones (Morimoto, R., Tissieres, A., and Georgopoulus, C., Eds.) (1994) pp 335-373, Cold Spring Harbor Laboratory Press, Cold Spring Harbor, NY.
ii. Artl A, Marsche G, Lestavel S, Sattler W, Malle E. Role of serum amyloid A during metabolism of acute-phase HDL by macrophages. Arterioscler Thromb Vasc Biol. 20 (2000) 763-72.
iii. Bettelheim FA[1], Ansari R, Cheng QF, Zigler JS Jr. The mode of chaperoning of dithiothreitol-denatured alpha-lactalbumin by alpha-crystallin. Biochem Biophys Res Commun. 261 (1999) 292-7.
iv. Botto, M., Hawkins, P. N., Bickerstaff, M. C. M., Herbert, J., Bygrave, A. E., McBride, A., Hutchinson, W. L., Tenneni, G. A., Walport, M. J., and Pepys, M. B. Amyloid deposition is delayed in mice with targeted deletion of the serum amyloid P component gene. Nature. Medicine. 3 (1997) 855-860.

v. Caspers, G. J., Leunissen, J. A. and de Jong, W. W. J. The expanding small heat-shock protein family, and structure predictions of the conserved "alpha-crystallin domain". Mol. Evol. 40 (1995) 238-248.
vi. Creighton, T. E. and Jaenicke, R. Protein folding: junior chaperones. Curr. Biol. 3 (1993) 234.
vii. Das S, Raychaudhuri M, Sen U, Mukhopadhyay D. Functional implications of the conformational switch in AICD peptide upon binding to Grb2-SH2 domain. J Mol Biol. 414 (2011) 217-30.
viii. Ehrnsperger, M., Graber, S., Gaestel, M., and Buchner, Binding of non-native protein to Hsp25 during heat shock creates a reservoir of folding intermediates for reactivation. J. EMBO. J. 16 (1997) 221-229.
ix. Horwitz, J. A small heat shock protein stably binds heat-denatured model substrates and can maintain a substrate in a folding-competent state. Invest. Ophthalmol. Vis. Sci. 34 (1993) 10-22.
x. Jens Brodbeck, Jim McGuire, Zhaoping Liu, Anke Meyer-Franke, Maureen E. Balestra, Dah-eun Jeong, Mike Pleiss, Casey McComas, Fred Hess, David Witter, Scott Peterson, Matthew Childers, Mark Goulet, Nigel Liverton, Richard Hargreaves, Stephen Freedman§, Karl H. Weisgraber, Robert W. Mahley, and Yadong Huang. Structure-dependent Impairment of Intracellular Apolipoprotein E4 Trafficking and Its Detrimental Effects Are Rescued by Small-molecule Structure Correctors. The Journal Of Biological Chemistry. 286 (2011) 17217–17226.
xi. Kaplan, B., Hrncic, R., Murphy, C. L., Gallo, G., Weiss, D. T., and Solmon, A. Micro extraction and purification techniques applicable to chemical characterization of amyloid proteins in minute amounts of tissue. Methods. Enzymol. 309 (1999) 67-81.
xii. Katsuya Sato, Tsuyoshi Sugiyama, Takahiro Nagase, Yukio Kitade, and Hiroshi Ueda. Threonine 680 Phosphorylation of FLJ00018/PLEKHG2, a Rho Family-specific Guanine Nucleotide Exchange Factor, by Epidermal Growth Factor Receptor Signaling Regulates Cell morphology of Neuro-2a cells. J Biol Chem. 289 (2014) 10045-56.
xiii. Konstantinos Tsioras, Florentia Papastefanaki, Panagiotis K. Politis, Rebecca Matsas, Maria Gaitanou. Functional Interactions between BM88/Cend1, Ran-binding protein M and Dyrk1B kinase affect cyclin D1 levels and cell cycle progression/exit in mouse neuroblastoma cells. PLoS One. 8 (2013) e82172.
xiv. Kwon B, Gamache T, Lee HK, Querfurth HW. Synergistic effects of β-amyloid and ceramide-induced insulin resistance on mitochondrial metabolism in neuronal cells. Biochim Biophys Acta. 1852 (2015)1810-1823.
xv. Kwon B, Gamache T, Lee HK, Querfurth HW. Synergistic effects of β-amyloid and ceramide-induced insulin resistance on mitochondrial metabolism in neuronal cells. Biochim Biophys Acta. 1852 (2015) 1810-1823.
xvi. Laemmli, U. K. Cleavage of structural proteins during the assembly of the head of bacteriophage T4. Nature. 227 (1970) 680-685.
xvii. Lee, G. J., Pokala, N., and Vierling, E. Structure and in vitro molecular chaperone activity of cytosolic small heat shock proteins from pea. J. Biol. Chem. 270 (1995) 10432-10438.
xviii. Lee, G. J., Roseman, A. M., Saibil, H. R., and Vierling E. A small heat shock protein stably binds heat-denatured model substrates and can maintain a substrate in a folding-competent state. EMBO J. 16 (1997) 659-671.
xix. Lindner, R. A., Kapur, A., and Carver, J. A. The interaction of the molecular chaperone, alpha-crystallin, with molten globule states of bovine alpha-lactalbumin. J. Biol. Chem. 44 (1997) 27722-27729.
xx. Linke, R. P., Bock, V., Valet, G., and Rothe, G. Inhibition of the oxidative burst response of N-formyl peptide-stimulated neutrophils by serum amyloid-A protein. Biochem. Biophys. Res. Commun. 176 (1991) 1100-1105.
xxi. Lorimer, G. A quantitative assessment of the role of the chaperonin proteins in protein folding in-vivo. FASEB. J. 10 (1996) 3-9.
xxii. Lowry Oh, Rosebrough Nj, Farr Al, Randall RJ. Protein measurement with the Folin phenol reagent. J. Biol. Chem. 193 (1951) 665-675.
xxiii. Luthra, M. and Balasubramanian, D. Nonenzymatic glycation alters protein structure and stability. A study of two eye lens Crystallin. J. Biol. Chem. 268 (1993) 18119-18127.
xxiv. Maria Manczak, Marcus J. Calkins and P. Hemachandra Reddy. Impaired mitochondrial dynamics and abnormal interaction of amyloid beta with mitochondrial protein Drp1 in neurons from patients with Alzheimer's disease: implications for neuronal damage. Human Molecular Genetics. 20 (2011) 2495–2509.
xxv. Panagiotis K. Politis, Dimitra Thomaidou and Rebecca Matsas. Coordination of cell cycle exit and differentiation of neuronal progenitors. Cell Cycle. 7 (2008) 691-697.
xxvi. Parsell, D. A. and Lindquist, S. The function of heat-shock proteins in stress tolerance: degradation and reactivation of damaged proteins. Annu. Rev. Genet. 27 (1993) 437-496.
xxvii. Preciado-Patt, L., Levartowsky, D., Pras, M., Hershkoviz, R., Lider, O., and Fridkin, M. Inhibition of cell adhesion to glycoproteins of the extracellular matrix by peptides corresponding to serum amyloid A. Toward understanding the physiological role of an enigmatic protein. Eur. J. Biochem. 223 (1994) 35-42.
xxviii. Raychaudhuri M[1], Mukhopadhyay D. Grb2-mediated alteration in the trafficking of AbetaPP: insights from Grb2-AICD interaction. J Alzheimers Dis. 20 (2011) 275-92.
xxix. Rousset Vincent Kindler, Conrad Hauser Jean-François Arrighi, and Michela Rebsamen Françoise. Lipopolysaccharide, TNF- a, and Contact Blood-Derived Dendritic Cells Induced by Protein Kinase in the Maturation of Human A Critical Role for p38 Mitogen-Activated. J Immunol. 166 (2001) 3837-3845.
xxx. Savolainen MH, Yan X, Myöhänen TT, Huttunen HJ. Prolyl oligopeptidase enhances α-synuclein dimerization via direct protein-protein interaction. J Biol Chem. 290 (2015) 5117-26.
xxxi. Walter, S. Lorimer, G. H., and Schmid, F. X. A thermodynamic coupling mechanism for GroEL-mediated unfolding. Proc. Natl. Acad. Sci. U.S.A. 93 (1996) 9425-9430.

Annexure

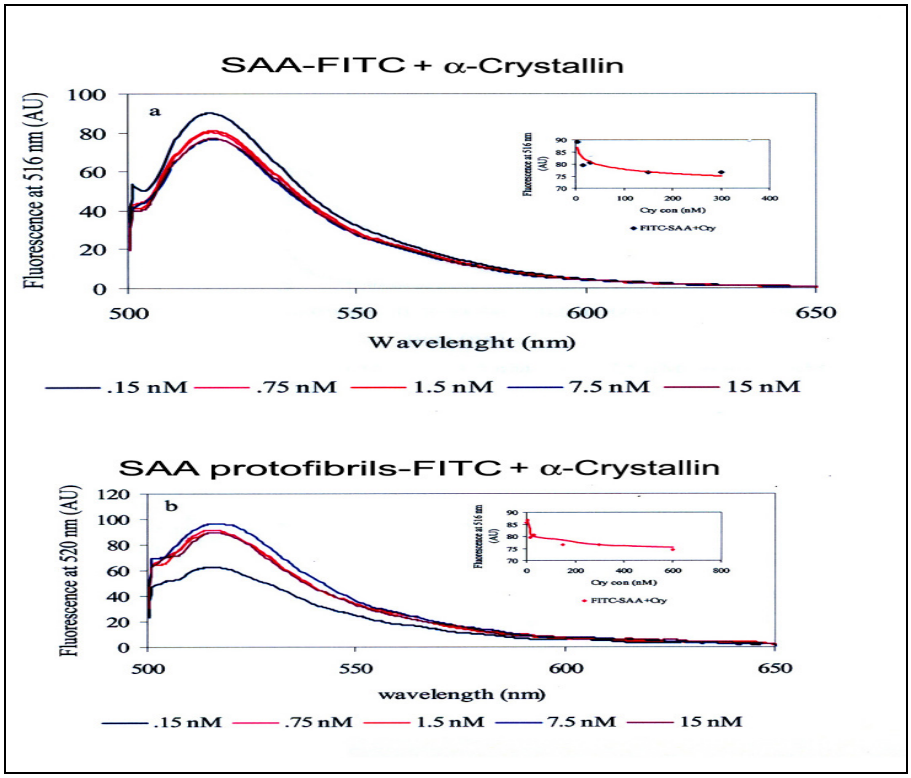

Figure 1: Fluorescence spectra of SAA-FITC (a) SAA-FITC (2.5 mM) with increasing concentration of (0.15-15 nM) -αB-Crystallin and insert plot shows concentration Vs Fluorescence, (b) SAA-FITC protofibrils (2.5 mM) with increasing concentration (0.15-15 nM) αB-Crystallin and insert plot shows concentration Vs Fluorescence.

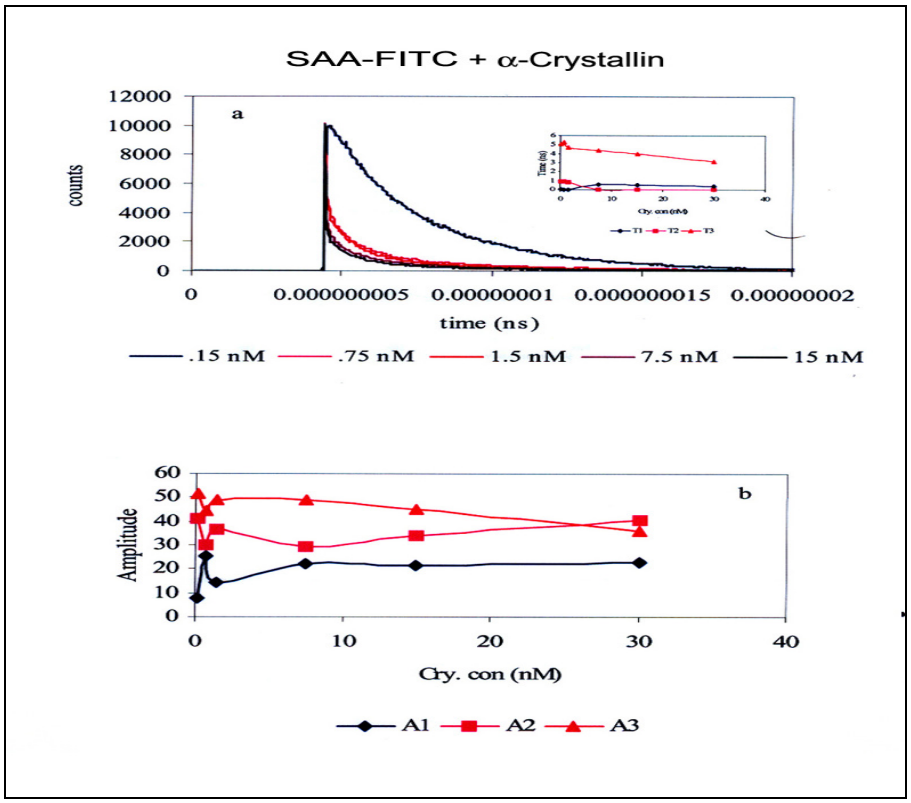

Figure 2: Life time measurement fluorescence decay of SAA-FITC (a) SAA-FITC (2.5 mM) with increasing concentration of (0.15-15 nM) αB-Crystallin and insert plot shows concentration Vs time, (b) plot shows concentration Vs amplitude.

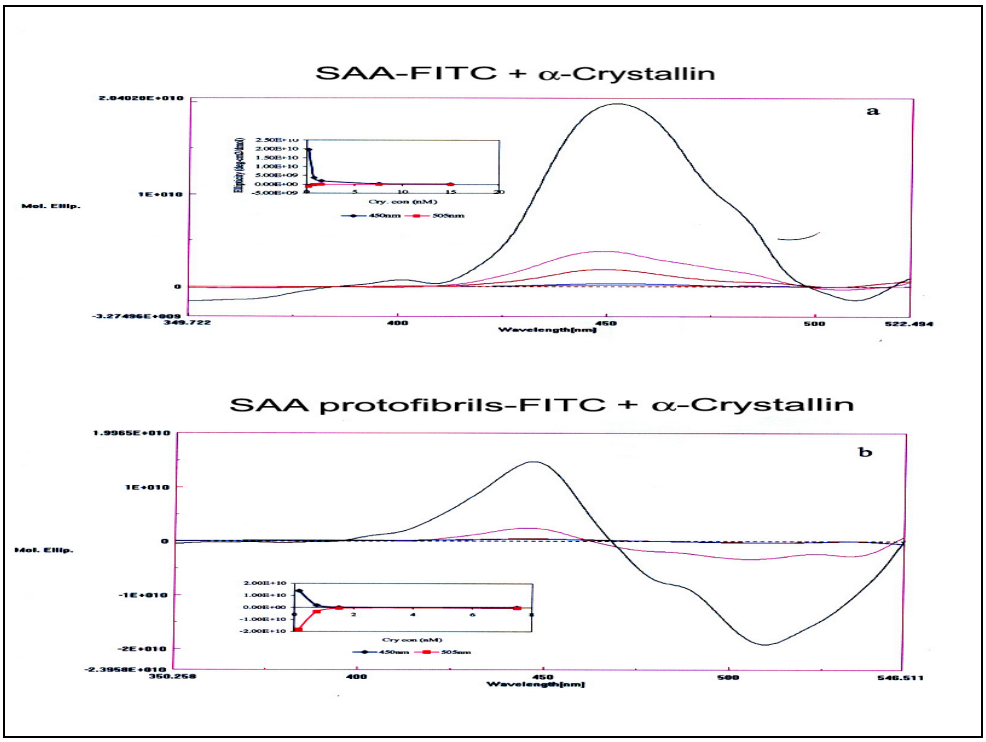

Figure 3: CD spectra of SAA-FITC (a) SAA-FITC (2.5 mM) with increasing concentration of (0.15-15 nM) αB-Crystallin and insert plot shows concentration Vs ellipticity at 450 and 505 nm, (b) SAA-FITC protofibrils (2.5 mM) with increasing concentration (0.15-15 nM) αB-Crystallin and insert plot shows concentration Vs ellipticity at 450 and 505 nm.

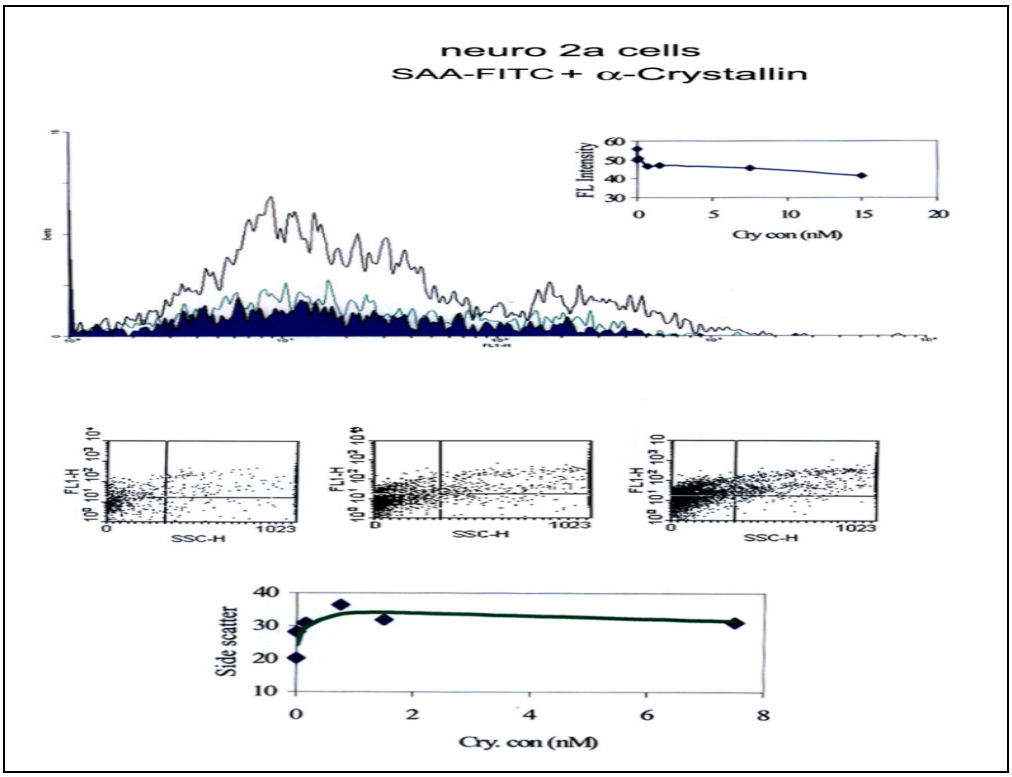

Figure 4: Effect of αB-Crystallin on SAA-FITC binding to mouse neuro 2a cells (a) histogram shows filled curve control cells, black curve (6.25 mM) SAA-FITC, green curve shows addition of (0.75 nM) αB-Crystallin and insert plot shows increasing concentration of αB-Crystallin (0.15-15 nM) Vs mean fluorescence (b) side scatter dot plot of neuro 2a cells and incubated with SAA-FITC (2.5 mM) (c) SAA-FITC with (0.15-15 nM) αB-Crystallin, (d) plot shows αB-Crystallin concentration Vs side scatter (upper right).

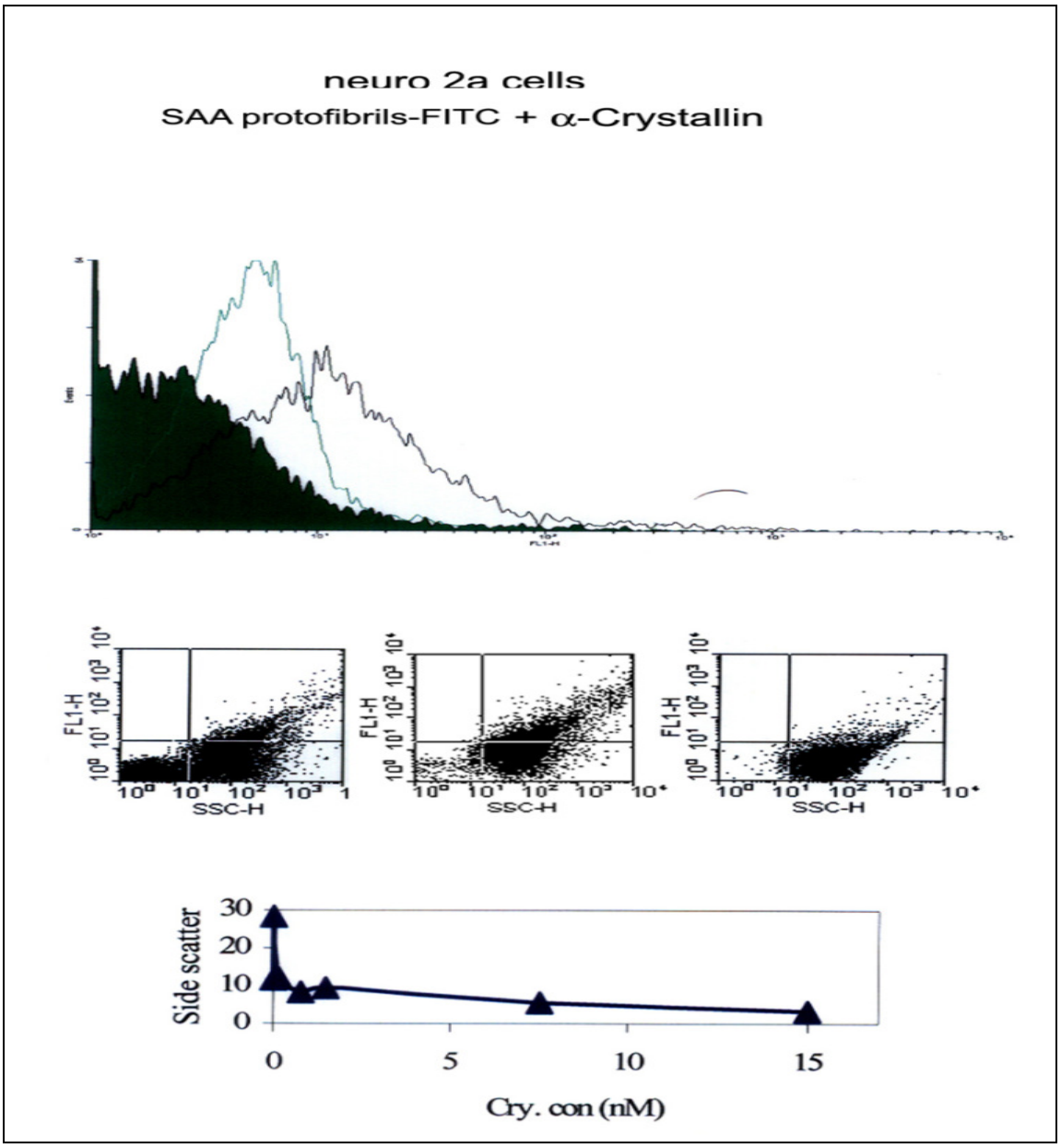

Figure 5: Effect of αB-Crystallin on SAA protofibrils-FITC binding to mouse neuro 2a cells (a) histogram shows filled curve control cells, black curve (6.25 mM) SAA protofibrils-FITC, green curve shows addition of (0.75 nM) αB-Crystallin and insert plot shows increasing concentration of αB-Crystallin (0.15-15 nM) Vs mean fluorescence (b) side scatter dot plot of neuro 2a cells and incubated with SAA-FITC (2.5 mM) (c) SAA protofibrils-FITC with (0.15-15 nM) αB-Crystallin, (d) plot shows αB-Crystallin concentration Vs side scatter (upper right).